OPEN ACCESS

Original research

Iatrogenic air embolism: influence of air bubble size on cerebral infarctions in an experimental in vivo and numerical simulation model

Tabea C Schaefer,[1,2] Svenja Greive,[1] Claas Bierwisch,[3] Shoya Mohseni-Mofidi,[3] Sabine Heiland,[1] Martin Kramer,[2] Markus A Möhlenbruch,[1] Martin Bendszus,[1] Dominik F Vollherbst [1]

► Additional supplemental material is published online only. To view, please visit the journal online (http://dx.doi.org/10.1136/jnis-2023-020739).

[1]Department of Neuroradiology, Heidelberg University Hospital, Heidelberg, Germany
[2]Department of Veterinary Clinical Sciences, Small Animal Clinic, Justus-Liebig-University Giessen, Giessen, Germany
[3]Fraunhofer IWM, Freiburg, Germany

Correspondence to
Dr Dominik F Vollherbst; dominik.vollherbst@med.uni-heidelberg.de

Received 28 June 2023
Accepted 10 August 2023
Published Online First 6 September 2023

To cite: Schaefer TC, Greive S, Bierwisch C, *et al*. *J NeuroIntervent Surg* 2024;**16**:1036–1041.

ABSTRACT

Background Cerebral infarctions resulting from iatrogenic air embolism (AE), mainly caused by small air bubbles, are a well-known and often overlooked event in endovascular interventions. Despite their significance, the underlying pathophysiology remains largely unclear.

Methods In 24 rats, AEs were induced using a microcatheter, positioned in the carotid artery via femoral access. Rats were divided into two study groups, based on the size of the bubbles (85 and 120 µm) and two sub-groups, differing in air volume (0.39 and 0.64 µl). Ultra-high-field magnetic resonance imaging (MRI) was performed 1.5 hours after intervention. MRI findings including the number, single volume and total volume of the infarctions were assessed. A software-based numerical simulation was performed to qualitatively assess the microvascular pathomechanisms.

Results In the study groups 22 of 24 rats (92%) revealed cerebral infarctions. The number of infarctions per rat was higher for the smaller bubbles, for the lower (medians: 5 vs 3; p=0.049) and higher air volume sub-groups (medians: 6 vs 4; p=0.012). Correspondingly, total infarction volume was higher for the smaller bubbles (1.67 vs 0.5 mm³; p=0.042). Simulations confirmed the results of the experiments and suggested that fusion of microbubbles to larger bubbles is the underlying pathomechanism of vascular occlusions.

Conclusion In iatrogenic AE, the size of the bubbles can have a major impact on the number and total volume of cerebral infarctions. These findings can help to better understand the pathophysiology of this frequent, often underestimated adverse event in endovascular interventions.

WHAT IS ALREADY KNOWN ON THIS TOPIC

⇒ Cerebral infarctions caused by iatrogenic air embolism during endovascular interventions are a known risk, but the underlying pathophysiology remains largely unclear.

WHAT THIS STUDY ADDS

⇒ In this systematic experimental study, it was shown that the air bubble size has a major influence on the number and volume of infarctions. This could be confirmed and explained by software-based numerical simulation.

HOW THIS STUDY MIGHT AFFECT RESEARCH AND PRACTICE

⇒ Through a better understanding of the pathophysiology of iatrogenic air embolism, prophylactic and therapeutic strategies can be developed based on these findings.

INTRODUCTION

Iatrogenic air embolism (AE) to the brain is a frequent, often underrated event in a variety of frequently performed endovascular interventions at the proximal aorta, the aortic arch and especially at the brain-supplying vessels, such as thoracic endovascular aortic repair (TEVAR), diagnostic cerebral angiographies, carotid artery stenting (CAS), and hemorrhagic or ischemic stroke treatments.[1–3]

Cerebral air embolism is of particular importance because of the poor collateralization of the terminal cerebral vasculature, the relatively short ischemic tolerance of brain parenchyma and the fact that even small infarctions in eloquent areas can lead to disabling ischemic strokes. The brain infarctions resulting from microemboli (gaseous or solid), which can be detected in magnetic resonance imaging (MRI), mostly as small punctuate lesions in diffusion-weighted imaging (DWI), are observed in up to 46% after cardiac procedures and can reach up to 67% after the implantation of flow diverters to treat intracranial aneurysms.[4 5] The origin of these DWI lesions, however, is often not clear and they can also be explained by solid microemboli. Nevertheless, AEs are considered to be a major contributor to these ischemic lesions.[1 2 6 7] This assumption is supported by the observation that the majority of embolic events during carotid angiograms occur during catheter flushing and injection of contrast material and not during navigation of the wires and catheters[8] and by studies using transcranial Doppler measurements showing that most embolic signals during TEVAR, carotid endarterectomy and CAS are gaseous.[6 9] While most of the aforementioned studies assessed DWI lesions of any origin, a recent study directly assessed air embolisms using CT in patients receiving cerebral angiography for acute ischemic stroke treatment. The study found an air embolism rate of 16%.[10]

The infarctions caused by AE are often clinically silent, but rarely they can lead to ischemic strokes, ranging from subtle motoric or neurocognitive impairments to disabling cerebral infarctions.[11 12]

Despite the high relevance of this adverse event, there is only little research on this field and the pathophysiology of ischemia due to AE and pathomechanisms of AEs are only poorly understood. It is known and obvious that the larger the applied air volume, the higher and larger the cerebral infarctions.[11] But apart from that, only little is known on factors influencing the cerebral damage by iatrogenic AE.

The aim of this study was to investigate the impact of the size of air bubbles on cerebral infarctions in a novel experimental in vivo model.

MATERIAL AND METHODS

Generation and detection of air bubbles

Air bubbles were produced and automatically measured in real time using an established model which was described previously in the literature.[13] With the aid of a microfluidic channel system (MCS) and a microfluidic pump, air bubbles were produced precisely and reproducibly. Bubble size could be influenced and regulated by the height and width of the MCS and by the pressures for liquid and air, which can be adjusted on the microfluidic pump.

In this study, we aimed to generate air bubbles with a target size of 85 µm and 120 µm, respectively. For the 85 µm bubbles, a channel dimension of 11 µm × 64 µm was used with pressures of 600 mbar (liquid) and 300 mbar (air). To produce the 120 µm bubbles we used 25 µm × 72 µm channels with pressures of 350 mbar (liquid) and 250 mbar (air).

Study groups

The design of the study groups is summarized in table 1. A total of 27 Wistar rats were used in this study. Twenty-four rats were allocated to the study groups (equal sex distribution in each group; average weight: 350 g) and three rats served as the control group. The study groups consisted of 12 rats each with an air bubble size of 85 µm and 120 µm, respectively, and a total of four sub-groups of six animals, differing in the volume of induced air (high volume: 0.64 µl and low volume: 0.39 µl) and thus the number of induced air bubbles. When converted by brain mass (rat: 2 g, human: 1450 g), this corresponds to 0.28 mL and 0.47 mL in a human. In all groups, the site of application of the air bubbles was the left common carotid artery (CCA). The rats in the control group were already used in a previous work.

Animal procedure

All experiments were performed in accordance with the Guide for the Care and Use of Laboratory Animals (Directive 2010/63/EU of the European Parliament). State Animal Care and Ethics Committee approval was obtained (registry number: 35–9185.81/G-183/20).

The rats were anesthetized with an intraperitoneal injection of 100 mg/kg ketamin (Ketamin 10%, Pharmanovo, Austria) and 5 mg/kg xylazine (Xylariem, Ecuphar GmbH, Germany). Between the endovascular procedure and the MRI, the rats were observed for behavioral changes, paresis or other signs of neurological damage. During MRI anesthesia was performed using isoflurane (Isofluran CP 1 mL/mL, CP-Pharma,Germany) with an initiation dose of 4% and a maintenance dose of 1 to 2%.

Endovascular procedure

Catheterization of the CCA was performed via the femoral artery using the Seldinger technique. After surgical exposure and incision of the vessel, a 26 G peripheral catheter (BD Neoflon, Heidelberg, Germany) was introduced into the femoral artery, following the insertion of a 0.014-inch microguidewire (Traxcess 14; MicroVention, Aliso Viejo; USA). After positioning the guidewire in the abdominal aorta, the 26 G catheter was removed. Afterwards a 156 cm/0.0165-inch microcatheter (Headway Duo; MicroVention) was inserted over the guidewire. The catheter was then positioned in the left CCA using the microguidewire. A manually modified syringe-catheter interface adapter was used to contact the hub of the microcatheter and the outlet tube of the MCS to inject the air bubbles. Afterwards either 1200 bubbles with a size of 85 µm (Group 85L), 2000 bubbles with a size of 85 µm (Group 85H), 426 bubbles with a size of 120 µm (Group 120L), or 711 bubbles with a size of 120 µm (Group 120H) were injected into the vascular system (duration of injection: 5 s; injection speed: 0.1 mL/s). After the air bubbles were injected the microcatheter was removed, the vessel was ligated, and the skin was stitched up with a continuous suture. In the rats in the control group, the microcatheter was also advanced into the left CCA and a diluted contrast agent without air bubbles was injected. All procedures were carried out under the fluoroscopic guidance (ARTIS icono or SIREMOBIL Compact L; Siemens Healthineers, Erlangen, Germany) and

Table 1 Study groups and summary of the quantitative results

Study group	Group 85			Group 120		
Sub-group	Group 85L	Group 85H	P-values	Group 120L	Group 120H	P-values
Air bubble size	85 µm	85 µm	–	120 µm	120 µm	–
Air volume	0.39 µl	0.64 µl	–	0.39 µl	0.64 µl	–
Air bubble number	1200	1200	–	426	711	–
Number of infarctions	5.0 (3.5; 5.0)	3.0 (0.0; 3.0)	0.049	6 (5.75; 6)	4 (3.5; 4)	0.012
Volume of infarctions* (mm³)	0.32 (0.16; 0.58)	0.3 (0.17; 0.66)	0.274	0.2 (0.11; 0.32)	0.24 (0.14; 0.4)	0.419
Total infarction volume† (mm³)	1.67 (0.71; 6.47)	0.5 (0; 0.9)	0.042	2.16 (1.54; 6.47)	1.1 (0.94; 5.13)	>0999

Quantitative data are presented as medians with interquartile range (median (first quartile; third quartile)).
*Volume of the single infarctions.
†Total infarction volume per rat.

under continuous flush of the catheter with saline. No heparin was added to the flush to minimize factors which could potentially influence the resulting cerebral alterations.

MRI

MRI was performed using a 9.4 Tesla small animal MR system (Bruker Biospec 94/20; Bruker Biospin, Ettlingen, Germany) 1 hour after the endovascular procedure. The following MRI sequences were performed: 3-dimensional time-of-flight (TOF) angiography, T2-weighted sequences (with 0.5 mm and 0.1 mm slice thickness, respectively), diffusion-weighted imaging (DWI) sequences, T1-weighted sequences before and after the application of a contrast agent, and a susceptibility-weighted sequence. T2-weighted sequences were performed as the first and last sequence within the protocol to improve the rate of detection of brain infarctions and other signal abnormalities. For contrast enhanced sequences 0.2 mmol/kg body weight of gadoteric acid (Dotarem; Guerbet, Villepinte, France) was administered intravenously via a venous tail vein catheter.

Study goals

The goal of our study was to investigate the influence of the air bubble size on the number and size of ischemic brain infarctions using two different volumes of air. For this purpose, the following data was collected and compared: the number of infarctions per rat, the volume of the respective infarctions, the total infarction volume per rat and the infarct pattern assessed in MRI using T2-weighted and DWI sequences.

Semi-automated segmentation of each infarction was carried out in T2 weighted 3D sequences 1.5 hours after induction of the air bubbles using the Medical Imaging Interaction Toolkit (MITK; German Cancer Research Center (DKFZ), Heidelberg, Germany) by TS and DFV with 2 and 9 years of experience in diagnostic radiology, respectively. Furthermore, MRI sequences were evaluated regarding visualization of intravascular or intracerebral air, vessel occlusions or other abnormal changes.

Statistics

GraphPad Prism (La Jolla, USA; version: 7.04) was used for this statistical analysis. Quantitative data are presented as medians with interquartile range (median (first quartile; third quartile)). To evaluate statistical differences between the study groups (Group 85L vs Group 120L; Group 85H vs Group 120H), the ANOVA test was performed. A P-value of 0.05 was defined as the threshold for statistical significance. P-values should be interpreted descriptively.

Simulation

Using the numerical simulation software SimPARTIX, designed to analyze the transient dynamics of multi-physics systems, the behavior of air bubbles within a vascular model was investigated independent of the in vivo studies. The virtual model consisted of a vascular network, originating from one vessel with 400 µm diameter, which branches dichotomously four times (diameters after the first, second, third and fourth branching: 320, 256, 205 and 164 µm, respectively), resembling the vascular network of the brain-supplying vessel of the rat. These diameters were selected as they are similar to the diameters of the internal carotid artery (ICA) and its branches (eg, anterior and middle cerebral artery) in the rat.[14]

The numerical simulations are based on the smoothed particle hydrodynamics method.[15] A multiphase scheme is used to stabilize the density difference within the flowing media.[16] Blood is modeled as a homogenized Newtonian fluid with a density of 1060 kg/m^3 and a dynamic viscosity of 3.5 mPa·s. The respective interface tensions of blood/air, blood/wall and air/wall are 56 mN/m, 10 mN/m and 70 mN/m which results in complete wetting of the vascular walls by the blood, that is, a contact angle between blood and wall of zero degrees.

The spatial resolution of the simulations is 10 µm while the temporal resolution is 0.5 µs. Simulations were performed using a number of 50 bubbles with a diameter of 85 µm and 25 bubbles with a diameter of 120 µm analogous to the in vivo experiments. The flow is driven by a pressure gradient of 60 kPa/m which is numerically expressed as a volumetric force acting on the blood and air.

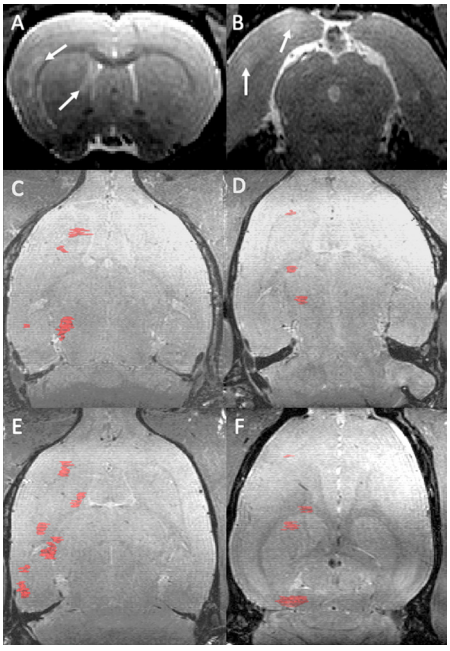

Figure 1 Findings in MRI. Infarctions induced by iatrogenic air embolism were visible as T2-hyperintense lesions (A; example from Group 85H) with corresponding diffusion restriction (B; example from Group 120H). Colored volume renderings (in red) of the infarctions after semi-automated segmentation show the distribution of the ischemic lesions, for example rats from Group 85L (C), Group 120L (D), group 85H (E) and Group 120H (F). Note the higher number of infarctions for the smaller air bubbles.

RESULTS

All procedures were performed as planned. No adverse events occurred during the interventions. During the short time between the endovascular procedure and MRI, in which the rats were awake, no behavioral changes or neurological symptoms were observed.

Imaging findings

Imaging findings are summarized in figure 1. Infarctions in MRI were detected as T2-hyperintense areas with corresponding diffusion restriction. In TOF-angiography no occlusion of cerebral vessels was observed and susceptibility-weighted sequences did not show any signal alterations being consistent with intravascular or intraparenchymal air or blood.

Number of infarctions

The numbers of infarctions are summarized in table 1 and illustrated in figure 2. Cerebral infarctions were detected in 22 of 24

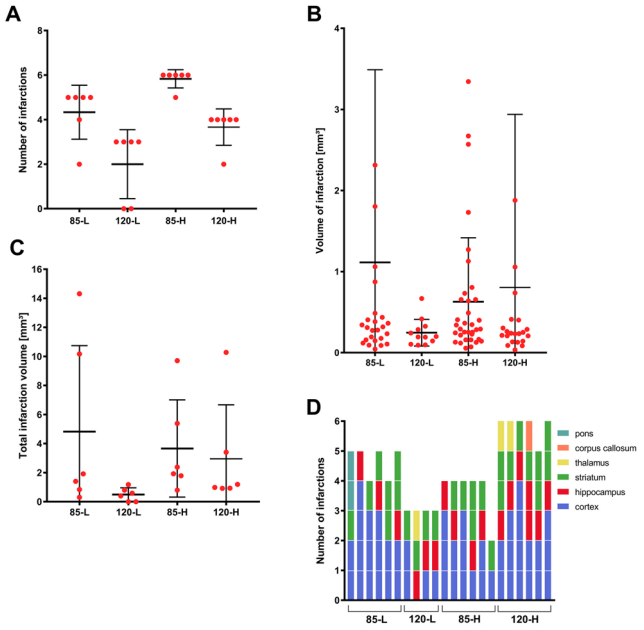

Figure 2 Illustration of the number of infarctions, infarct volume, total infarction volume and distribution of brain infarctions. Number of infarctions (A), volume of the single infarctions (B) and total infarction volume (C) are illustrated as scattered dot plots (lines indicating median and interquartile range). The analysis of the distribution of the brain infarction (D) did not show differences regarding size or volume of the air bubbles.

(92%) rats in the study groups and in no rats in the control group. In rats with infarctions the number ranged from 2 to 6. Both rats without infarctions were in Group 120L. The number of infarctions was higher for the smaller air bubbles both for the lower (medians: 5 vs 3; p=0.049) and the higher (medians: 6 vs 4; p=0.012) air volume. The lowest number of infarctions (median: 3) was observed in Group 120L while the highest number of infarctions (median: 6) was observed in Group 85H.

Volume of infarctions

The volumes of infarctions as well as the total infarction volumes are summarized in table 1 and illustrated in figure 2. The volume of the single infarctions was not different between the study groups. The volumes of the cerebral infarctions ranged from a small punctuate infarction with 0.05 mm^3 to a larger infarction with 10.18 mm^3. The total infarction volume was higher for the 85 µm air bubbles only for the groups with lower air volume (medians: 1.7 vs 0.5; p=0.042).

Infarction pattern

The distribution of the infarctions is illustrated in figure 2D. Most infarctions appeared in the cortex, striatum and hippocampus, revealing an embolic pattern. The incidence of the respective areas in rats with infarction is as follows: 96% (21/22 rats) for cortex, 91% (20/22 rats) for striatum and 73% (16/22 rats) for hippocampus. There was a similar distribution of infarcts within and between the study groups.

Simulation

The videos of the numerical simulations are available as online supplemental materials. A simulation using 85 µm bubble diameter is summarized in figure 3A, and a comparison between a case using bubble diameters of 85 µm and 120 µm, respectively, is shown in figure 3B.

The simulations showed that the fusion of multiple small air bubbles leads to the development of larger bubbles. The fusion occurs especially at branchings where the blood velocity decreases because of continuity along the increasing total flow cross section. The large bubbles eventually occlude the terminal vessels. This finding was observed both for the simulations using 85 and 120 µm bubbles. Comparing the simulations between these different bubble diameters, using 85 µm bubbles, eight terminal vessels were occluded, while this was observed for only six terminal vessels using 120 µm bubbles.

DISCUSSION

In this study investigating iatrogenic air embolism in an experimental in vivo model, we systematically analyzed the influence of air bubble size at two different air volumes. It could be demonstrated, that the size of the air bubbles has a major impact on the number of the resulting brain infarctions, while the size of the single infarctions and their distribution is similar comparing different air bubble sizes.

Endovascular interventions at vessels supplying the brain (eg, carotid and intracranial arteries) or upstream of them (eg, aortic valve and aortic arch) belong to the most frequently performed vascular procedures worldwide. Many efforts are being made to analyze, avoid and prevent complications during these interventions.[17] Actions to prevent iatrogenic AE include a continuous flush of the catheters which are being used, careful visual inspection of syringes used for injection, air filters and specific flushing systems for TEVAR devices.[1 17 18] These efforts can reduce the rate of AE, but as mentioned in the introduction, AEs still occur frequently.

The work published by Furlow in 1982 was one of the first experimental studies on air embolisms using air emboli of 5 µl injected directly into the ICA using a direct cervical access.[19] This work can be regarded as a pioneer study in this research field as several later studies basically adapted Furlow's air embolism model. In most of these later studies, air bubbles were produced simply by manual mixing of liquid and air in a syringe.[20 21] While the volume of air is known using this technique, the number of air bubbles and their size remain unknown, which significantly limits the conclusions which can be made based on studies using such bubbles.

In contrast to previous experimental studies on AE, where mostly a direct surgical access to the cerebral vessels was obtained, our study uses an endovascular approach via the femoral artery, resembling endovascular interventions in clinical practice.[20 22] Furthermore, the size and number of air bubbles and the volume of air are similar to the situation of air embolism in human medicine during catheter-based interventions.[23 24]

The reason for the selection of the air bubble sizes in this study was that 85 µm is a common size of so-called micro air bubbles, which make up the majority of air bubbles occuring during catheter-based procedures.[23 25] The other bubble size of 120 µm was chosen to have a sufficient difference in size to the micro air bubble and to use larger bubbles that are still small enough to enter the vasculature unnoticed in everyday practice. The volume and number of bubbles was derived from clinical studies which showed that in cardiac surgeries, such as TEVAR procedures, the total volume of air injected ranges between 0.0003 and 0.79 mL and an average number of 1600 per patient.[24 25] As stated in the material and methods section, the selected air volume in this study of 0.39 µl (L-groups) and 0.64 µl (H-groups) corresponds to 0.28 mL and 0.47 mL in humans converted by brain volume.

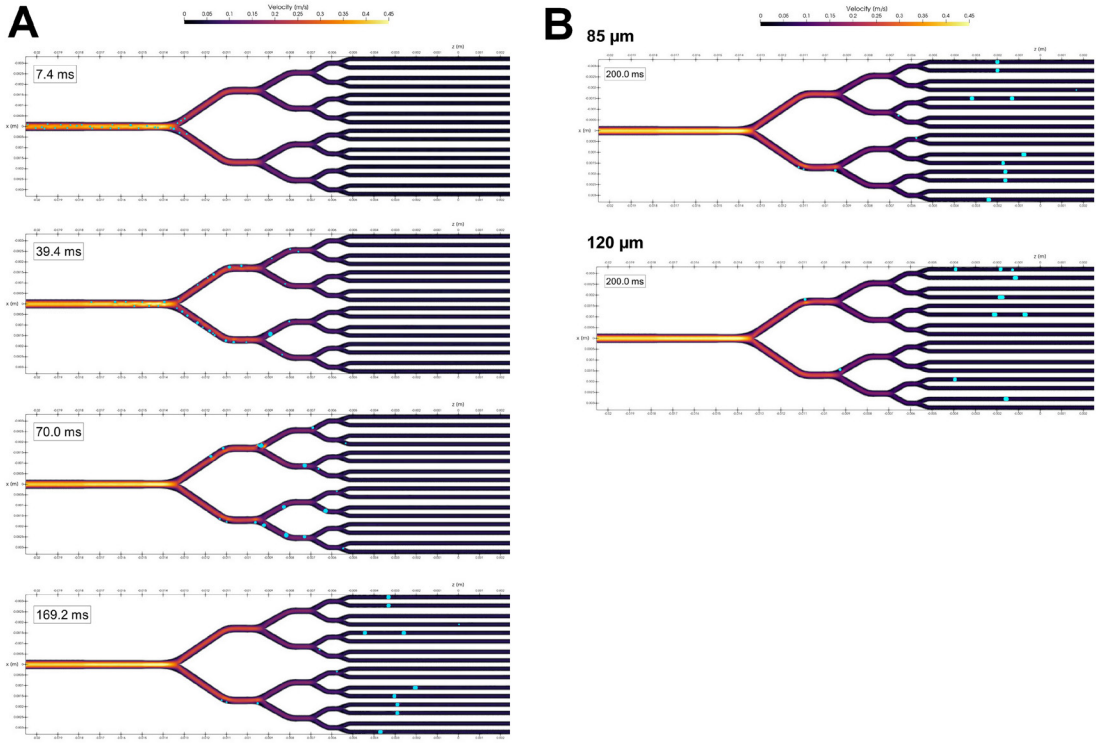

Figure 3 Illustration of the software-based simulation. (A) illustrates the vascular model and shows different points in time of the simulation using 85 µm air bubbles. At 7.4 ms the 85 µm air bubbles are not yet fused and enter the first branching. During the flow through the vascular model (39.4 ms and 70.0 ms), especially at the branchings, small bubbles fuse to larger ones, which eventually cause occlusions of the terminal vessels. A few bubbles adhere to the vessel walls within the model. (B) shows the end of simulations using 85 µm and 120 µm air bubbles. At this point, eight of the terminal vessels are occluded, while using 120 µm bubbles, occlusion in only six vessels was observed. This qualitative analysis is in line with the findings of the in vivo experiments.

We observed a higher number of infarctions for the smaller air bubbles. Additionally to the known fact that these micro air bubbles are more frequent, our results indicate that the smaller air bubbles are also more harmful than larger ones.

The in vivo findings could also be confirmed in the experimental simulations. In vivo studies of the behavior of air bubbles in the cervical and intracranial vasculature are practically not feasible and models for experimental in vitro analyses do not exist. A numerical simulation model, as it was used in our study, can help to understand the pathophysiology of these air bubbles causing cerebral infarctions. The validity of the numerical simulation scheme has been demonstrated in other scientific non-medical fields using several benchmark cases for multiphase flows and capillary phenomena.[26 27] Despite the value of the simulation, several factors had to be assumed, such as the condition of the blood or the interface tensions. Gravity, which might play a considerable role in air bubble behavior, was not considered thus limiting the reliability of the conclusions based on the simulation.

A recent study by Li *et al*, which used in vivo and in vitro microfluidic experiments, also focused on the mechanism of vascular occlusion caused by air embolism in small vessels.[28] They found that a clot, which could not be simulated in our software-based model, is always found at the tail of a moving air bubble, and that the flow field around the bubble plays a major role in vascular occlusion.

A possible explanation for the higher number of infarctions for the smaller air bubbles in our study is the gas-liquid endothelial interface. This can be an important factor influencing the extent of vessel occlusion by the bubbles themselves, activation of the blood clotting cascade, as well as the induction of inflammatory response.[29] With the same total air volume but smaller bubbles, a larger surface area and thus a larger gas-fluid-endothelial interface can be assumed. Calculating the total surface area of the injected bubbles, the 85 µm have a 41% larger surface compared with the 120 µm bubbles. This can be a crucial factor which leads to the higher degree of tissue damage for the bubbles with smaller diameter.

Another possible explanation for the higher number of infarctions for the smaller air bubbles is the relation of the size of the air bubbles to the terminal vasculature. It can be assumed that smaller air bubbles circulate deeper into the terminal vasculature, where there is only little or no collateralization of the terminal vessels, while larger bubbles get stuck more proximal where collateralization is possible.[11] In this regard, also the geometry of air bubbles seems to be an important factor as it influences the residence time of intravascular bubbles, which again influences the absorption time and can thus play a major role in the development of infarctions.[30]

An interesting finding, which is also evident in human studies, is that, irrespective of the volume of air and the size of the bubbles, multiple small air bubbles cause only a relatively low number of infarctions. According to the software-based simulation, which was performed in our study, this phenomenon can be explained by the fusion of many single bubbles into larger bubbles, clogging larger blood vessels, resulting in infarctions which can be detected in MRI.

Besides the larger number of infarctions, which was observed for the smaller bubbles, the total infarction volume was higher in one sub-group despite similar volumes of the single infarctions. The larger total infarction volume, which was observed for the

sub-group with a smaller air volume is most likely explained by the higher number of infarctions.

As mentioned in the introduction, DWI lesions after endovascular procedures can explained by AE but also by solid emboli. In our study, the probability of infarctions caused by other emboli than air can be regarded as very low, as no infarctions were detected in the control group, in which catheters were also navigated into the CCA, however, without the injection of air.

In our study, the impact of the air bubbles was only systematically assessed in MRI and not in specific neurobehavioral tests as rats were only awake for a short time after air bubble injection and they were finalized after the imaging. These tests could have delivered further relevant results and should be performed in future studies with sufficient survival times.

We acknowledge that this study has noteworthy limitations. The number of experiments per study group was small. However, the findings were consistent within the individual study groups. We only used air bubbles with a size of 85 µm or 120 µm and injected only either 1200 or 2000 bubbles. The injection of smaller or larger air bubbles or different numbers of air bubbles could have led to different results. Another limitation is that the microcatheter for air bubble injection had to be placed within the CCA and not the ICA due to the small size of the ICA in relation to the microcatheter. Air entering the external carotid artery, and thus not entering the cerebral vessels, could have biased the results. Furthermore, the transfer of an experimental animal model and of a software-based simulation on clinical practice is generally limited.

CONCLUSION

In this experimental in vivo model investigating iatrogenic air embolism, the size of the bubbles had a major impact on the number and total volume of cerebral infarctions. These findings can help to better understand the pathophysiology, prevention and ultimately treatment of this frequent, often underestimated adverse event in endovascular interventions.

Contributors TCS, MB and DFV designed the study. TCS, SG and DFV performed the in vivo experiments. CB and SMM performed the simulations. All authors analyzed and interpreted data for the work. TCS, SH, MB and DFV drafted the manuscript. All authors approved the final manuscript. DFV is the guarantor of this work.

Funding The authors have not declared a specific grant for this research from any funding agency in the public, commercial or not-for-profit sectors.

Competing interests MB reports the following conflicts of interest outside the present work: board membership: DSMB Vascular MAM has received consulting honoraria, speaker honoraria, and travel support outside this work from Codman, Covidien/Medtronic, MicroVention, Phenox, and Stryker. MB reports board membership: DSMB Vascular Dynamics; consultancy: Roche, Guerbet, Codman; grants/grants pending: DFG, Hopp Foundation, Novartis, Siemens, Guerbet, Stryker, Covidien; payment for lectures (including service on speakers bureaus): Novartis, Roche, Guerbet, Teva, Bayer, Codman. DFV reports consultancy for Medtronic and paid lectures for Cerenovus, and a research grant by MicroVention (unrelated to this work). The other authors declare that they do not have any conflicts of interest.

Patient consent for publication Not applicable.

Ethics approval Not applicable.

Provenance and peer review Not commissioned; externally peer reviewed.

Data availability statement All data relevant to the study are included in the article or uploaded as supplementary information. Not appicable.

ORCID iD

Dominik F Vollherbst http://orcid.org/0000-0002-8992-4757

REFERENCES

1 Bendszus M, Koltzenburg M, Bartsch AJ, *et al*. Heparin and air filters reduce embolic events caused by intra-arterial cerebral angiography: a prospective, randomized trial. *Circulation* 2004;110:2210–5.
2 Bendszus M, Koltzenburg M, Burger R, *et al*. Silent embolism in diagnostic cerebral angiography and neurointerventional procedures: a prospective study. *Lancet* 1999;354:1594–7.
3 Charbonneau P, Kölbel T, Rohlffs F, *et al*. Silent brain infarction after endovascular arch procedures: preliminary results from the STEP registry. *Eur J Vasc Endovasc Surg* 2021;61:239–45.
4 Wiberg S, Vedel AG, Holmgaard F, *et al*. Lack of association between gaseous microembolisms assessed by a single detection device and cerebral complications in cardiac surgery patients. *J Cardiothorac Vasc Anesth* 2020;34:1496–503.
5 Bond KM, Brinjikji W, Murad MH, *et al*. Diffusion-weighted imaging-detected ischemic lesions following endovascular treatment of cerebral aneurysms: a systematic review and meta-analysis. *AJNR Am J Neuroradiol* 2017;38:304–9.
6 Grover G, Perera AH, Hamady M, *et al*. Cerebral embolic protection in thoracic endovascular aortic repair. *J Vasc Surg* 2018;68:1656–66.
7 Perera AH, Rudarakanchana N, Monzon L, *et al*. Cerebral embolization, silent cerebral infarction and neurocognitive decline after thoracic endovascular aortic repair. *Br J Surg* 2018;105:366–78.
8 Dagirmanjian A, Davis DA, Rothfus WE, *et al*. Silent cerebral microemboli occurring during carotid angiography: frequency as determined with Doppler sonography. *AJR Am J Roentgenol* 1993;161:1037–40.
9 Skjelland M, Krohg-Sørensen K, Tennøe B, *et al*. Cerebral microemboli and brain injury during carotid artery endarterectomy and Stenting. *Stroke* 2009;40:230–4.
10 Huijberts I, Pinckaers FME, van Zwam WH, *et al*. Cerebral arterial air emboli on immediate post-endovascular treatment CT are associated with poor Short- and long-term clinical outcomes in acute ischaemic stroke patients. *J Neuroradiol* 2023.
11 Barak M, Katz Y. Microbubbles: pathophysiology and clinical implications. *Chest* 2005;128:2918–32.
12 van Hulst RA, Klein J, Lachmann B. Gas embolism: pathophysiology and treatment. *Clin Physiol Funct Imaging* 2003;23:237–46.
13 Schaefer TC, Greive S, Heiland S, *et al*. Investigation of experimental endovascular air embolisms using a new model for the generation and detection of highly calibrated micro air bubbles. *J Endovasc Ther* 2023;30:461–70.
14 Herz RC, Jonker M, Verheul HB, *et al*. Middle cerebral artery occlusion in Wistar and Fischer-344 rats: functional and morphological assessment of the model. *J Cereb Blood Flow Metab* 1996;16:296–302.
15 Monaghan JJ. Smoothed particle hydrodynamics. *Rep Prog Phys* 2005;68:1703–59.
16 Colagrossi A, Landrini M. Numerical simulation of interfacial flows by smoothed particle hydrodynamics. *J Comput Phys* 2003;191:448–75.
17 McCarthy CJ, Behravesh S, Naidu SG, *et al*. Air embolism: practical tips for prevention and treatment. *J Clin Med* 2016;5:93.
18 Rohlffs F, Trepte C, Ivancev K, *et al*. Air embolism during TEVAR: liquid perfluorocarbon absorbs carbon dioxide in a combined flushing technique and decreases the amount of gas released from thoracic stent-grafts during deployment in an experimental setting. *J Endovasc Ther* 2019;26:76–80.
19 Furlow TW. Experimental air embolism of the brain: an analysis of the technique in the rat. *Stroke* 1982;13:847–52.
20 Jungwirth B, Kellermann K, Blobner M, *et al*. Cerebral air emboli differentially alter outcome after cardiopulmonary bypass in rats compared with normal circulation. *Anesthesiology* 2007;107:768–75.
21 Weenink RP, Hollmann MW, Stevens MF, *et al*. Cerebral arterial gas embolism in swine. comparison of two sites for air injection. *J Neurosci Methods* 2011;194:336–41.
22 Gerriets T, Walberer M, Nedelmann M, *et al*. A rat model for cerebral air microembolisation. *J Neurosci Methods* 2010;190:10–3.
23 Chung EML, Banahan C, Patel N, *et al*. Size distribution of air bubbles entering the brain during cardiac surgery. *PLoS One* 2015;10:e0122166.
24 Rohlffs F, Tsilimparis N, Saleptsis V, *et al*. Air embolism during TEVAR: carbon dioxide flushing decreases the amount of gas released from thoracic stent-grafts during deployment. *J Endovasc Ther* 2017;24:84–8.
25 Makaloski V, Rohlffs F, Spanos K, *et al*. Bubble counter for measurement of air bubbles during thoracic stent-graft deployment in a flow model. *J Surg Res* 2018;232:121–7.
26 Polfer P, Kraft T, Bierwisch C. Suspension modeling using smoothed particle hydrodynamics: accuracy of the viscosity formulation and the suspended body dynamics. *Applied Mathematical Modelling* 2016;40:2606–18.
27 Bierwisch C. Consistent thermo-capillarity and thermal boundary conditions for single-phase smoothed particle hydrodynamics. *Materials (Basel)* 2021;14:4530.
28 Li Z, Li G, Li Y, *et al*. Flow field around bubbles on formation of air embolism in small vessels. *Proc Natl Acad Sci USA* 2021;118:26.
29 Juenemann M, Yeniguen M, Schleicher N, *et al*. Impact of bubble size in a rat model of cerebral air microembolization. *J Cardiothorac Surg* 2013;8:198.
30 Branger AB, Eckmann DM. Theoretical and experimental Intravascular gas embolism absorption dynamics. *J Appl Physiol (1985)* 1999;87:1287–95.